NANO LETTERS

Letter

pubs.acs.org/NanoLett

Large Thermoelectric Figure-of-Merits from SiGe Nanowires by Simultaneously Measuring Electrical and Thermal Transport Properties

Eun Kyung Lee,[†,●] Liang Yin,[‡,●] Yongjin Lee,[§,●] Jong Woon Lee,[∥] Sang Jin Lee,[†] Junho Lee,[⊥] Seung Nam Cha,[†] Dongmok Whang,[∥] Gyeong S. Hwang,[§] Kedar Hippalgaonkar,[¶] Arun Majumdar,[■] Choongho Yu,*[,‡] Byoung Lyong Choi,*[,†] Jong Min Kim,*[,†,▲] and Kinam Kim[#]

[†]Frontier Research Laboratory, Samsung Advanced Institute of Technology, Samsung Electronics, Yongin, Kyunggi-do 446-712, South Korea

[‡]Department of Mechanical Engineering, Texas A&M University, College Station, Texas 77843, United States

[§]Department of Chemical Engineering, University of Texas, Austin, Texas 78712, United States

[∥]School of Advanced Materials Science and Engineering, Sungkyunkwan University, Suwon, Kyunggi-do, South Korea

[⊥]Analytical Engineering Group, Samsung Advanced Institute of Technology, Samsung Electronics, Yongin, Kyunggi-do 446-712, South Korea

[#]Samsung Advanced Institute of Technology, Samsung Electronics, Yongin, Kyunggi-do 446-712, South Korea

[¶]Department of Mechanical Engineering, University of California, Berkeley, California 94720, United States

[■]ARPA-E, U.S. Department of Energy, 1000 Independence Avenue, Washington, DC 20585, United States

Supporting Information

ABSTRACT: The strongly correlated thermoelectric properties have been a major hurdle for high-performance thermoelectric energy conversion. One possible approach to avoid such correlation is to suppress phonon transport by scattering at the surface of confined nanowire structures. However, phonon characteristic lengths are broad in crystalline solids, which makes nanowires insufficient to fully suppress heat transport. Here, we employed Si−Ge alloy as well as nanowire structures to maximize the depletion of heat-carrying phonons. This results in a thermal conductivity as low as ∼1.2 W/m-K at 450 K, showing a large thermoelectric figure-of-merit (ZT) of ∼0.46 compared with those of SiGe bulks and even ZT over 2 at 800 K theoretically. All thermoelectric properties were "simultaneously" measured from the same nanowires to facilitate accurate ZT measurements. The surface-boundary scattering is prominent when the nanowire diameter is over ∼100 nm, whereas alloying plays a more important role in suppressing phonon transport for smaller ones.

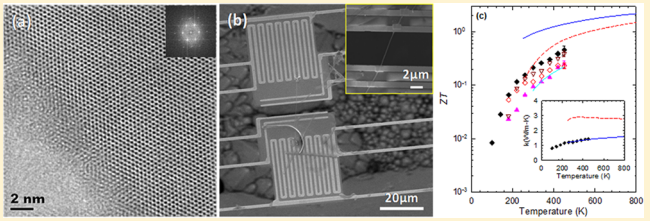

KEYWORDS: *Simultaneous measurement, thermal conductivity reduction, alloy scattering, boundary scattering*

Thermoelectric devices directly convert heat into electricity or vice versa through simple structures without moving parts. Such features have attracted significant research efforts to improve their efficiencies, which are typically described by the thermoelectric figure-of-merit (ZT). However, thermoelectric properties, such as thermopower (or the Seebeck coefficient) (S), electrical conductivity (σ), electronic thermal conductivity ($k_{electron}$), and lattice thermal conductivity (k_{phonon}), that comprise $ZT = S^2\sigma T/(k_{electron} + k_{phonon})$, where T is temperature, are strongly correlated, making ZT improvement difficult. For instance, it has been difficult to reduce thermal conductivity while electrical properties are maintained or improved. Recent results suggest that this hurdle may be overcome by suppressing phonon transport (so as to reduce k_{phonon}) without significantly altering other properties.[1−3] In crystalline solids, phonon characteristic lengths such as wavelengths and mean free paths are often much longer than those of electrons, making it possible to selectively confine phonons rather than electrons. Particularly, one-dimensional nanowire structures are very effective for suppressing the phonon contribution due to scattering at the wire boundaries. For instance, the thermal conductivities that have been measured from Si nanowires are significantly decreased in comparison to that of a bulk crystalline Si.[4] Nevertheless, the phonons whose characteristic lengths are smaller than the nanowire diameters are likely to be less affected; however, it is

Received: February 12, 2012
Revised: April 30, 2012
Published: May 1, 2012

impractical to reduce the diameter to a few nanometers or less in order to deplete short-length phonons. These phonons could be suppressed by introducing impurities or defects whose sizes are smaller than the nanowire diameters. It should be noted that electron transport may also be sensitive to impurities and defects in crystalline solids,[5] altering electrical conductivity and/or thermopower. Therefore, it is very important that all three properties, S, σ, and k ($= k_{electron} + k_{phonon}$) are obtained from the same nanowire so as to properly address the influence of various parameters including diameters, impurities, and defects on thermoelectric transport behaviors. In this work, we employed 6- to 86-atom % Ge in SiGe nanowires whose diameters ranged from 26 to 161 nm, and their S, σ, and k values were measured for the same nanowire. All structural information including diameter, length, crystallinity, oxide layer thickness, and Si/Ge concentration ratio was obtained from the nanowires that were used for the measurements. The highest ZT was ~0.46 at 450 K due to significantly decreased thermal conductivities, which were further investigated by using computational approaches based on nonequilibrium molecular dynamics (NEMD) and the Boltzmann transport equation. Furthermore, high temperature ZT values were estimated to be over 2, which suggests that the nanowire-based thermoelectrics may be viable for efficient energy conversion.

SiGe nanowires of excellent crystallinity were grown by the vapor−liquid−solid (VLS) method[6,7] (see Supporting Information), as demonstrated in Figure 1a by the high-resolution transmission electron micrograph (TEM). The spacing of the lattice fringes is 3.22 Å and the growth direction corresponds to $[\bar{1}1\bar{1}]$ from the selected area electron diffraction pattern. Table 1 depicts eight nanowires of different diameters, lengths, and compositions that were used in the measurements. Nanowires were bridged between two suspended membranes[8−11] on which four Pt electrodes were patterned as shown in the inset of Figure 1b. In order to reduce thermal contact resistance, Ni or Pt was deposited by using focused ion beam (FIB) (Figure 1b) or/and samples were annealed at 600 °C in a high vacuum environment (better than 10^{-6} Torr) or H_2 environment. The nickel deposition made the contact ohmic, as confirmed by linear current−voltage characteristics.

Figure 2 demonstrates the experimentally measured thermal conductivities of the SiGe alloy nanowires, which rapidly increased at low temperatures and then saturated at 1−2 W/m-K near room temperatures. These values are considerably lower than those of similar-diameter (56 and 22 nm) Si nanowires[4] grown by the VLS method as well as those of three-dimensional $Si_{0.9}Ge_{0.1}$ and $Si_{0.6}Ge_{0.4}$ bulk alloys.[12] Large thermal conductivity reductions up to ~30-fold obtained from the SiGe nanowires compared to the Si nanowire are likely to be derived from the scattering of phonons whose characteristic lengths are smaller than the nanowire diameters. Meanwhile, the low

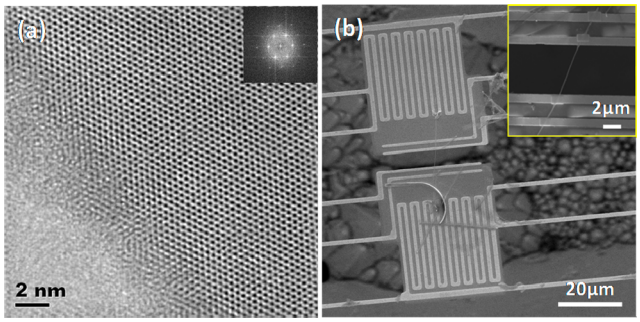

Figure 1. The morphology of SiGe nanowires and a microdevice for measuring thermoelectric properties. (a) A high-resolution TEM of a $Si_{0.9}Ge_{0.1}$ nanowire grown via the VLS method and a selected-area electron diffraction pattern in the inset. The growth direction of the nanowire is $[\bar{1}1\bar{1}]$. (b) A nanowire is bridged between two suspended membranes. The contacts were improved by using various methods including Ni or Pt depositions as shown in the inset.

Table 1. A List of the SiGe Nanowire Samples[a]

sample	length (μm)	diameter (nm)	oxide thickness (nm)	metal by FIB	annealing
$Si_{0.94}Ge_{0.06}$	5.7	56	0		Vac
$Si_{0.92}Ge_{0.08}$	6.3	97	0	Ni	H_2
$Si_{0.90}Ge_{0.10}$	5.6	45	0	Ni	H_2
$Si_{0.81}Ge_{0.19}$	5.0	62	0		Vac
$Si_{0.74}Ge_{0.26}$	11.6	26	0	Ni	H_2
$Si_{0.73}Ge_{0.27}$	5.3	26	2	Ni	H_2
$Si_{0.59}Ge_{0.41}$	5.2	65	2.8	Pt	
$Si_{0.14}Ge_{0.86}$	6.2	161	0		Vac

[a]The Si and Ge atomic ratios, lengths, and total diameters including oxide shells, and oxide layer thicknesses of the SiGe nanowires. The oxide thickness indicates the length of the amorphous oxide layers in the radial direction from the center axis. In order to minimize the contact resistance between the nanowires and microdevice membranes, Ni or Pt was deposited by using a FIB system, and/or annealing at 600 °C in vacuum (better than 10^{-6} Torr) or in an H_2 environment was performed.

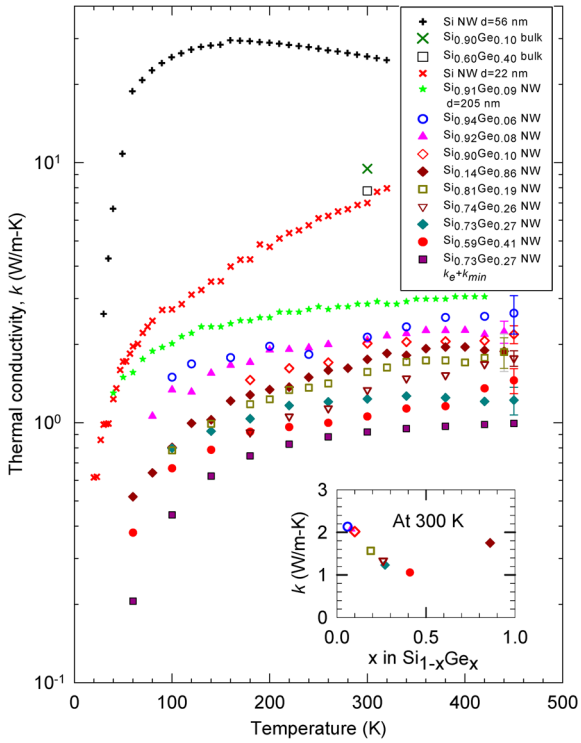

Figure 2. The thermal conductivities of the SiGe nanowires. The thermal conductivities of the SiGe nanowires listed in Table 1 are plotted with those of the previously reported samples including a 56 nm diameter Si nanowire,[4] a $Si_{0.9}Ge_{0.1}$ bulk,[12] a $Si_{0.6}Ge_{0.4}$ bulk,[12] a $Si_{0.91}Ge_{0.09}$ nanowire,[15] and the calculated summation of electronic (k_e) and minimum (k_{min}) thermal conductivities for the $Si_{0.74}Ge_{0.26}$ nanowire. The inset shows the thermal conductivities at 300 K of the SiGe nanowires that were measured in our study.

dx.doi.org/10.1021/nl300587u | Nano Lett. 2012, 12, 2918−2923

thermal conductivities, 1−2 W/m-K at 300 K, that were obtained for the SiGe "nanowires" in comparison to 7−8 W/m-K for "bulk" counterparts indicate that phonons with long characteristic lengths were deterred. These comparisons suggest two crucial information: (1) the phonons whose characteristic lengths are smaller than the wire diameter can be further scattered by alloying; (2) a large portion of heat is carried by phonons with long characteristic lengths in alloys. The scattering cross-section is proportional to $(d/\lambda)^4$ like the Rayleigh scattering,[13] where d and λ are, respectively, the characteristic lengths of impurities and phonons, making phonons with long characteristic lengths in alloys still important in heat transport due to small d/λ in alloys. In fact, calculation results[14] have also suggested that heat transport in bulk SiGe has large contributions from phonons with relatively long (up to micrometer scale) mean free paths. The boundary confinement effects are conspicuous for nanowires with relatively large diameters (205 nm $Si_{0.91}Ge_{0.09}$[15] and 97 nm $Si_{0.92}Ge_{0.08}$); however, it appears that smaller diameters (56 nm $Si_{0.94}Ge_{0.06}$ and 45 nm $Si_{0.90}Ge_{0.10}$) do not further influence the thermal conductivity (atomic ratio of Si/Ge ∼ 0.9:0.1).

On the other hand, when Ge concentrations were raised from 6% ($Si_{0.94}Ge_{0.06}$) to 19% ($Si_{0.81}Ge_{0.19}$) or 41% ($Si_{0.59}Ge_{0.41}$) with relatively constant diameters (56, 62, and 65 nm, respectively), the thermal conductivities were further suppressed, reaching ∼1 W/m-K near room temperature. The thermal conductivities of smaller diameter (26 nm) but with less Ge samples, $Si_{0.74}Ge_{0.26}$ and $Si_{0.73}Ge_{0.27}$, fit more or less between those of $Si_{0.81}Ge_{0.19}$ and $Si_{0.59}Ge_{0.41}$. The thermal conductivities at 300 K in our experimental results also suggest strong influence of the Ge concentration, as shown in the inset of Figure 2. It is noticeable that the $Si_{0.73}Ge_{0.27}$ nanowire has very low thermal conductivities that are only ∼0.2 W/m-K higher than the summation of the electronic thermal conductivity (k_e) and the minimum lattice thermal conductivity (k_{min}). k_e was obtained from the Wiedemann Franz law with a Lorenz number of 2.44×10^{-8} ΩK^{-2} and k_{min} was calculated with the constant speed of sound over the temperature range by using the model proposed by Cahill et al.[16]

We intentionally bridged the two wires on microdevices whose gaps between the membranes are different so that the suspended portions are respectively 5.3 and 11.6 μm for $Si_{0.73}Ge_{0.27}$ and $Si_{0.74}Ge_{0.26}$ (samples were simultaneously synthesized). The thermal conductances of $Si_{0.73}Ge_{0.27}$ were approximately twice those of $Si_{0.74}Ge_{0.26}$. Since we measured thermal conductance (G) and then multiplied the geometrical factors to obtain the thermal conductivity ($k = G \times L/A_c$, where A_c and L are the cross-sectional area and length of the wire, respectively), thermal contact resistances between the wires and membranes are not likely to significantly influence the measurement results. The total thermal resistances from the measurements (across the wire length) are on the order of 10^8 K/W or higher, whereas the contact resistances are estimated to be smaller than $\sim 5 \times 10^6$ K/W. The contact resistance was obtained by assuming the contact width and thermal conductivity are, respectively, 10 nm and 0.5−1 W/m-K at 150 and 300 K.[13] The contact widths were also underestimated because the contact area deposited by focused ion beam is typically greater than 0.5×1 μm^2. Furthermore, we tested different approaches to improve the thermal contacts, such as Pt or Ni depositions on four (or two) contacts with/without thermal annealing or only vacuum annealing (no deposition), for similar nanowires, $Si_{0.94}Ge_{0.06}$, $Si_{0.92}Ge_{0.08}$, and $Si_{0.90}Ge_{0.10}$ so as to exclude the possibility of dominant effects from contact resistances. We did not observe any noticeable differences depending on the aforementioned contact treatments.

Nonequilibrium molecular dynamics (NEMD) simulations were also performed using the large-scale atomic/molecular massively parallel simulator (LAMMPS)[17] to better understand the relative contributions of the Si−Ge alloying and nanowire surface effects at the nanowire boundary to thermal resistivity. In order to examine their relative roles, we computed k values for the nanowire systems and compared them to those of periodic systems. For the rectangular-shaped simulation domain, periodic boundary conditions were imposed only in the axial (z) direction for the nanowire systems and in all three (x, y, and z) directions for the reference periodic systems. The cross-section consists of 10 × 10 (or 20 × 20) units, while the domain was axially divided into a number of thin shells, and each of which was one-unit thick (corresponding to 400 (or 1600) atoms). The heat source and heat sink layers were one-unit thick, and the total axial length of the rectangular domain was set to 122 units. We used a general form of the Stillinger−Weber (SW) potential function[18] that includes two-body (stretching) and three-body (bending) terms. Therein, the SW parameters that were necessary to fit the density-functional theory (DFT) results of the restoring forces that act on the local lattice distortion-associated constituent atoms are summarized in the Supporting Information.

According to Matthiessen's rule, the total phonon scattering rate (τ^{-1}) can be expressed as the sum of alloy (τ_a^{-1}), surface (τ_s^{-1}), intrinsic (predominantly phonon−phonon (τ_{p-p}^{-1})), and periodicity (τ_h^{-1}, due to the heat source and heat sink) contributions. Hence, the scattering rates for nanowire and periodic systems are given by $\tau_{NW}^{-1} = \tau_a^{-1} + \tau_s^{-1} + \tau_{p-p}^{-1} + \tau_h^{-1}$ and $\tau_P^{-1} = \tau_a^{-1} + \tau_{p-p}^{-1} + \tau_h^{-1}$, respectively. Although the thermal resistance directly depends on the scattering rate, we computed the relative thermal resistance ($\gamma = R_{NW}/R_P$) of the nanowire (R_{NW}) with respect to the periodic (R_P) systems considered. As summarized in Figure 3, our calculations show that the predicted nanowire resistances for pure Si and Ge samples are about twice that of the periodic cases. However, γ rapidly decreases as Si and Ge are alloyed and nearly falls to a valley

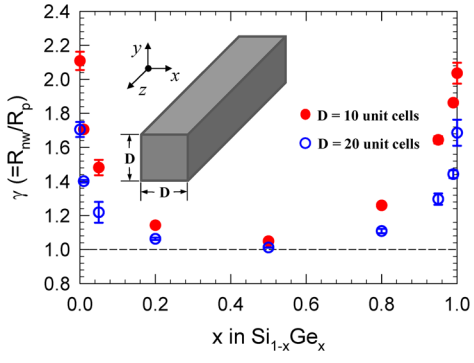

Figure 3. The relative thermal resistance ($\gamma = R_{NW}/R_P$) between the nanowire (R_{NW}) and periodic (R_P) SiGe alloy systems. For the nanowire case, two different cross-sectional areas are considered (10 × 10 and 20 × 20 unit cells, as indicated by filled and open circles, respectively). Periodic boundary conditions are imposed only in the axial (z) direction for the nanowire systems and in all three (x, y, and z) directions for the reference periodic system. For each system, eight independent NEMD simulations with different initial velocity distributions were performed to obtain good statistics.

dx.doi.org/10.1021/nl300587u | Nano Lett. 2012, 12, 2918−2923

plateau between 20−80% of Ge. These results suggest that alloy scattering in nanowires becomes the prevailing scattering mechanism, which is consistent with the experimental results that are depicted in Figure 2, rather than surface scattering for the case of small diameter nanowires; however, the possibility of overestimating the extent of alloy scattering in MD simulations cannot be excluded. Our study also demonstrates the reduction of the surface-scattering effect as a function of increasing the nanowire cross-section, 10 × 10 versus 20 × 20 units.

The electrical properties and ZT of the $Si_{0.92}Ge_{0.08}$, $Si_{0.90}Ge_{0.10}$, $Si_{0.74}Ge_{0.26}$, and $Si_{0.73}Ge_{0.27}$ nanowires are plotted in Figure 4 with those of a radioisotope thermoelectric generator (RTG) sample that was typically used for NASA space flight[19] for comparison. Unlike thermal conductivity, the electrical conductivities are less sensitive to diameter and Ge concentration, presumably due to short electron mean free paths. The electrical conductivities of the nanowires are inferior to those of the RTG bulk sample. On the other hand, the absolute thermopower values from $Si_{0.90}Ge_{0.10}$ and $Si_{0.74}Ge_{0.26}$ are larger than those from the RTG, making the power factors from nanowires close to those of the RTG. With much lower thermal conductivities from the nanowires than the bulk, $Si_{0.73}Ge_{0.27}$ shows a large ZT improvement of up to ∼0.46 at 450 K, which is twice that of the RTG, as shown in Figure 4c. This result is over 50% higher than that of the p-type nanostructured-bulk SiGe alloy[20] and ∼30% higher than that of the n-type nanostructured-bulk SiGe alloy,[21] respectively. It should be noted that errors associated with geometrical parameters are not involved. These parameters are not necessary to obtain ZT as long as all σ, S, and k are measured from the same sample.

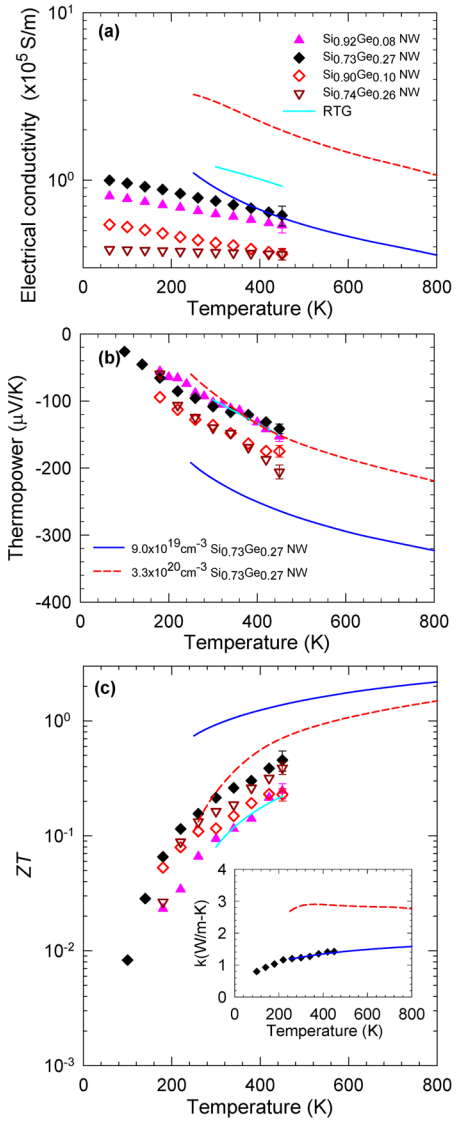

Figure 4. Simultaneously measured (60−450 K) and theoretically calculated (250−800 K) electrical conductivity, thermopower, and the figure-of-merit (ZT) of the SiGe nanowires. (a) Electrical conductivity, (b) thermopower, and (c) ZT values are plotted for $Si_{0.92}Ge_{0.08}$, $Si_{0.90}Ge_{0.10}$, $Si_{0.74}Ge_{0.26}$, and $Si_{0.73}Ge_{0.27}$ with those of a bulk SiGe RTG[19] as reference values. Calculated results were obtained with two different carrier densities, 9.0 × 10^{19} (blue solid line) and 3.3 × 10^{20} cm^{-3} (red broken line) for $Si_{0.73}Ge_{0.27}$.

Furthermore, even higher ZT values up to 2.2 at 800 K were estimated from calculated electrical conductivity, thermopower, and lattice thermal conductivity based on the Boltzmann transport equation up to 800 K, as plotted with lines in Figure 4 (see Supporting Information for details). The electrical properties were calculated by using the model for "bulk" SiGe proposed by Vining,[22] considering both electrons and holes as well as two major scattering mechanisms due to acoustic phonons and ionized impurities. The electron mean free paths are estimated to be shorter than the wire diameter, which is likely to make the electrical transport properties of bulks similar to those of the nanowires. In Figure 4a,b, the blue solid and red broken lines, respectively, represent electrical properties of bulk SiGe when either electrical conductivity or thermopower is similar to those of the $Si_{0.73}Ge_{0.27}$ nanowire. Corresponding carrier densities were found to be 9.0 × 10^{19} and 3.3 × 10^{20} cm^{-3} for the blue and red lines, respectively. The discrepancies in the experimental values from the nanowires and those from bulk SiGe (calculation) are presumably due to inferior electrical properties of the nanowires compared to those of bulks. The confined structure often makes electron transport very sensitive to impurities, nonuniformly distributed dopants,[23,24] and/or deactivated dopants.[25] For example, electrical conductivity may significantly drops even with high carrier concentrations when a small cylindrical section in the middle (along the nanowire axial direction) of the nanowire is electrically less conducting.

High-temperature thermal conductivities up to 800 K were obtained by calculating both lattice and electronic thermal conductivities. The lattice and electronic thermal conductivities were calculated with the Callaway model modified by Mingo[26] and Morelli et al.,[27] and the Wiedemann Franz law, respectively. The relatively high thermal conductivity with the higher carrier density (3.3 × 10^{20} cm^{-3}) is due to the electronic contribution to the total thermal conductivity. In order to fit our experimental data, the cutoff frequency was used as an adjustable parameter when normal phonon scattering, phonon−phonon umklapp scattering, impurity scattering, electron−phonon scattering, and scattering from the wire boundary were considered. The projected ZT value at 450 K is 1.4, higher than that of Bi−Te based state-of-the-art alloys, and is even much higher, 2.2 at 800 K when Si is alloyed with Ge by 27%, under the assumption that the electrical properties of nanowires are similar to those of bulk SiGe.

Upon further optimizing the nanowire synthesis process, it may be possible to obtain electrical properties close to those of

dx.doi.org/10.1021/nl300587u | Nano Lett. 2012, 12, 2918−2923

bulks with a high concentration of phosphorus doping and followed by thermal annealing. When Si is oxidized due to the presence of oxygen, it has been found that phosphorus can diffuse into Si (i.e., segregates from SiO_2 shells) and Ge as well as accumulate at the interface between Si and SiO_2.[23,24,28] As shown in the Supporting Information, energy dispersive spectroscopy profiles show the presence of phosphorus in the core region of our samples. Upon optimized synthesis and/or thermal annealing processes, it may be possible that dopants are more uniformly distributed without deactivated dopants, resulting in improved electrical properties.

In conclusion, we report a large improvement in ZT values, experimentally ~0.46 at 450 K and computationally 2.2 at 800 K, from SiGe nanowires. The experimental results were obtained by "simultaneously" measuring thermal conductivity, electrical conductivity, and thermopower. It is crucial to obtain all three properties from the same nanowire since their compositions, crystallinity, and thermoelectric properties might vary considerably even for the samples that are grown at the same time. The ZT improvement is attributed to remarkable thermal conductivity reductions, which are thought to derive from the effective scattering of a broad range of phonons by alloying Si with Ge as well as by limiting phonon transport within the nanowire diameters. Surface boundary scattering is prominent when the nanowire diameter is ~100 nm or larger, whereas Ge alloying plays a more important role in suppressing the thermal conductivity of smaller diameter samples. The additional phonon scattering in alloy nanowires might provide opportunities to use relatively large-diameter nanowires for maintaining the structural integrities required for building practical nanowire-based thermoelectric energy conversion devices in the future.

■ ASSOCIATED CONTENT

Supporting Information

Additional and comprehensive explanations associated with experimental procedures, TEM images, error analysis, and calculation results. This material is available free of charge via the Internet at http://pubs.acs.org.

■ AUTHOR INFORMATION

Corresponding Author

*E-mail: (C.Y.) chyu@tamu.edu; (B.L.C.) choibl@samsung.com; (J.M.K.) jong.kim@eng.ox.ac.uk.

Present Address

▲Department of Engineering Science, University of Oxford, Parks Road, Oxford, OX1 3PJ.

Author Contributions

●These authors contributed equally to this work.

Notes

The authors declare no competing financial interest.

■ ACKNOWLEDGMENTS

C.Y. and L.Y. acknowledge the financial support from the U.S. National Science Foundation (0854467), the U.S. Air Force Office of Scientific Research (FA9550-09-1-0609), and the Pioneer Research Center Program through the National Research Foundation of Korea (2011-0001645) funded by the Ministry of Education, Science, and Technology (MEST).

■ REFERENCES

(1) Poudel, B.; Hao, Q.; Ma, Y.; Lan, Y. C.; Minnich, A.; Yu, B.; Yan, X.; Wang, D. Z.; Muto, A.; Vashaee, D.; Chen, X. Y.; Liu, J. M.; Dresselhaus, M. S.; Chen, G.; Ren, Z. High-thermoelectric performance of nanostructured bismuth antimony telluride bulk alloys. *Science* **2008**, *320*, 634.

(2) Kim, W.; Zide, J.; Gossard, A.; Klenov, D.; Stemmer, S.; Shakouri, A.; Majumdar, A. Thermal conductivity reduction and thermoelectric figure of merit increase by embedding nanoparticles in crystalline semiconductors. *Phys. Rev. Lett.* **2006**, *96*, 045901.

(3) Hsu, K. F.; Loo, S.; Guo, F.; Chen, W.; Dyck, J. S.; Uher, C.; Hogan, T.; Polychroniadis, E. K.; Kanatzidis, M. G. Cubic AgPbmSbTe2+m: Bulk thermoelectric materials with high figure of merit. *Science* **2004**, *303*, 818.

(4) Li, D.; Wu, Y.; Kim, P.; Shi, L.; Yang, P.; Majumdar, A. Thermal conductivity of individual silicon nanowires. *Appl. Phys. Lett.* **2003**, *83*, 2934.

(5) Fischetti, M. V.; Laux, S. E. Band structure, deformation potentials, and carrier mobility in strained Si, Ge, and SiGe alloys. *J. Appl. Phys.* **1996**, *80*, 2234.

(6) Wagner, R. S.; Ellis, W. C. Vapor-liquid-solid mechanism of single crystal growth. *Appl. Phys. Lett.* **1964**, *4*, 89.

(7) Zhang, X.; Lew, K. K.; Nimmatoori, P.; Redwing, J. M.; Dickey, E. C. Diameter-Dependent Composition of Vapor−Liquid−Solid Grown $Si_{1-x}Ge_x$ Nanowires. *Nano Lett.* **2007**, *7*, 3241.

(8) Yu, C.; Saha, S.; Zhou, J. H.; Shi, L.; Cassell, A. M.; Cruden, B. A.; Ngo, Q.; Li, J. Thermal contact resistance and thermal conductivity of a carbon nanofiber. *J. Heat Transfer* **2006**, *128*, 234.

(9) Shi, L.; Li, D.; Yu, C.; Jang, W.; Kim, D.; Yao, Z.; Kim, P.; Majumdar, A. Measuring Thermal and Thermoelectric Properties of One-Dimensional Nanostructures Using a Microfabricated Device. *J. Heat Transfer* **2003**, *125*, 881.

(10) Zhou, F.; Moore, A. L.; Pettes, M. T.; Lee, Y.; Seol, J. H.; Ye, Q. L.; Rabenberg, L.; Shi, L. Effect of Growth Base Pressure on the Thermoelectric Properties of Indium Antimonide Nanowires. *J. Phys. D* **2010**, *43*, 025406.

(11) Yu, C.; Shi, L.; Yao, Z.; Li, D.; Majumdar, A. Thermal Conductance and Thermopower of an Individual Single-Wall Carbon Nanotube. *Nano Lett.* **2005**, *5*, 1842.

(12) Dismukes, J. P.; Ekstrom, L.; Steigmeier, E. F.; Kudman, I.; Beers, D. S. Thermal and Electrical Properties of Heavily Doped Ge-Si Alloys up to 1300 K. *J. Appl. Phys.* **1964**, *35*, 2899.

(13) Tien, C.-L.; Majumdar, A.; Gerner, F. M. *Microscale Energy Transport*; Taylor & Francis: Washington DC, 1998.

(14) Dames, C.; Chen, G. Thermal Conductivity of Nanostructured Thermoelectric Materials. In *Thermoelectrics Handbook: Macro to Nano*; Rowe, D., Ed.; Taylor & Francis Group: Wales, U.K., 2005.

(15) Kim, H.; Kim, I.; Choi, H. J.; Kim, W. Thermal conductivities of $Si_{1-x}Ge_x$ nanowires with different germanium concentrations and diameters. *Appl. Phys. Lett.* **2010**, *96*, 221105.

(16) Cahill, D. G.; Watson, S. K.; Pohl, R. O. Lower limit to the thermal conductivity of disordered crystals. *Phys. Rev. B* **1992**, *46*, 6131.

(17) Plimpton, S. Fast parallel algorithms for short-range molecular dynamics. *J. Comput. Phys.* **1995**, *117*, 1.

(18) Stillinger, F. H.; Weber, T. A. Computer simulation of local order in condensed phases of silicon. *Phys. Rev. B* **1985**, *31*, 5262.

(19) Abelson, R. D. Space Missions and Applications. In *CRC Handbook of Thermoelectrics*; Rowe, D. M., Ed.; CRC: Boca Raton, FL, 1995.

(20) Joshi, G.; Lee, H.; Lan, Y.; Wang, X.; Zhu, G.; Wang, D.; Gould, R. W.; Cuff, D. C.; Tang, M. Y.; Dresselhaus, M. S.; Chen, G.; Ren, Z. Enhanced Thermoelectric Figure-of-Merit in Nanostructured p-Type Silicon Germanium Bulk Alloys. *Nano Lett.* **2008**, *8*, 4670.

(21) Wang, X. W.; Lee, H.; Lan, Y. C.; Zhu, G. H.; Joshi, G.; Wang, D. Z.; Yang, J.; Muto, A. J.; Tang, M. Y.; Klatsky, J.; Song, S.; Dresselhaus, M. S.; Chen, G.; Ren, Z. F. Enhanced thermoelectric figure of merit in nanostructured n-type silicon germanium bulk alloy. *Appl. Phys. Lett.* **2008**, *93*, 193121.

(22) Vining, C. B. A model for the high-temperature transport properties of heavily doped n-type silicon-germanium alloys. *J. Appl. Phys.* **1991**, *69*, 331.
(23) Perea, D. E.; Hemesath, E. R.; Schwalbach, E. J.; Lensch-Falk, J. L.; Voorhees, P. W.; Lauhon, L. J. Direct measurement of dopant distribution in an individual vapour-liquid-solid nanowire. *Nat. Nanotechnol.* **2009**, *4*, 315.
(24) Koren, E.; Berkovitch, N.; Rosenwaks, Y. Measurement of Active Dopant Distribution and Diffusion in Individual Silicon Nanowires. *Nano Lett.* **2010**, *10*, 1163.
(25) Fair, R. B.; Tsai, J. C. C. A Quantitative Model for the Diffusion of Phosphorus in Silicon and the Emitter Dip Effect. *J. Electrochem. Soc.* **1977**, *124*, 1107.
(26) Mingo, N. Calculation of Si nanowire thermal conductivity using complete phonon dispersion relations. *Phys. Rev. B* **2003**, *68*, 113308.
(27) Morelli, D. T.; Heremans, J. P.; Slack, G. A. Estimation of the isotope effect on the lattice thermal conductivity of group IV and group III-V semiconductors. *Phys. Rev. B* **2002**, *66*, 195304.
(28) Fukata, N.; Ishida, S.; Yokono, S.; Takiguchi, R.; Chen, J.; Sekiguchi, T.; Murakami, K. Segregation Behaviors and Radial Distribution of Dopant Atoms in Silicon Nanowires. *Nano Lett.* **2011**, *11*, 651.